DOI: 10.1002/ejic.201000792

Titanium(IV)–Salan Catalysts for Asymmetric Sulfoxidation with Hydrogen Peroxide

Pedro Adão,[a] Fernando Avecilla,[b] Marcella Bonchio,[c] Mauro Carraro,[c] João Costa Pessoa,*[a] and Isabel Correia*[a]

Keywords: Titanium / Oxidation / Ionic liquids / Heterogeneous catalysis / Asymmetric catalysis

We report the synthesis and the solution and solid-phase characterization of several titanium(IV)–salan complexes. The structures of the ligands H_2sal(*R*,*R*-chan), H_2ovan(*S*,*S*-chan), and H_6pyr(*R*,*R*-chan)$^{4+}$·4Cl$^-$·H_2O were determined by single-crystal X-ray diffraction and their main features are compared and discussed. Single crystals suitable for X-ray diffraction studies were also obtained for [Ti$_4${sal(*R*,*R*-chan)}$_4$(μ-O)$_4$] and showed a tetranuclear core bearing μ-oxo bridges between the titanium atoms and the ligand wrapped around the Ti in a *fac-mer* geometry. The Ti–salan complexes were tested as catalysts in the benchmark oxidation of thioanisole with H_2O_2 as oxidant in organic solvents. High H_2O_2 conversion and moderate enantioselectivities (up to 51 % *ee*) were obtained. In an effort to perform greener catalysis the complexes were tested in selected ionic liquids with several oxidants. [Ti{5-MeO-sal(*R*,*R*-chan)}] was also covalently bound to a polystyrene matrix. *tert*-Butyl hydroperoxide was found to be the most suitable oxidant for use in ionic liquids (100 % conversion vs. 80 % with H_2O_2) and in general the Ti–salan complexes showed better activity in ILs at 25 °C although with reduced induced asymmetry (up to 18 % *ee*).

Introduction

The controlled catalytic oxidation of organic sulfides to sulfoxides remains a challenge because of the widespread application of sulfoxides in industry. For example, esomeprazole, which is produced industrially by a modified method developed by Kagan[1] and Modena[2] and their co-workers independently in 1984, was the third biggest-selling pharmaceutical drug in the world in 2005 (ca. 5.7 billion dollars in sales).[3] However, the reaction is performed in toxic and environmentally hazardous solvents like dichloromethane. Thus, our ultimate goal is to design and synthesize efficient titanium-based sulfoxidation catalysts that promote enantioselective oxygen transfer to prochiral sulfides when immobilized in recyclable phases such as ionic liquids or anchored on polymeric scaffolds such as cross-linked polystyrene.

The tetradentate diamino diphenolate ligands, also known as tetrahydrosalen or salan ligands, are attracting increasing interest due to their rich coordination chemistry.[4–8] They can be obtained from the reduction of salen precursors or by the reaction of the selected diamine with a 2,4-disubstituted phenol and formaldehyde in a modified Mannich reaction.[9] This class of ligands and their metal complexes present much higher resistance to hydrolysis than their salen counterparts,[10–13] which is very important when using a "green" solvent such as water or ionic liquids and/or a "green" oxidant such as aqueous hydrogen peroxide, or when anchored to cross-linked polystyrene.

Salan ligands lead to well-defined complexes that allow the tuning of the metal geometry and the electronic and steric properties by simply varying the ligand structure and substitution pattern. Salan-type ligands bind to early-transition metals often in a *fac-fac* (*cis*-α) geometry to form octahedral C_2-symmetric complexes with the two labile groups in a *cis* geometry.[4,5,7,8,14,15] When bound in this fashion, the nitrogen atoms of the salan ligand and the metal become stereogenic centers.

Titanium–salan complexes have been applied as catalysts in polymerization reactions,[6,15,16] in the alkylation of aldehydes,[8,17,18] and in asymmetric oxidation reactions. Most of the work with chiral Ti(salan) in epoxidation and sulfoxidation reactions has been performed by Katsuki and coworkers: Ti(salan) complexes were found to be efficient catalysts for asymmetric epoxidation reactions[19,20] with *ee* values higher than 90% when using aqueous H_2O_2 as the terminal oxidant. In the presence of phosphate buffer, the reactions of various conjugate olefins proceeded smoothly to afford the corresponding epoxides in high yields and with high enantioselectivities.[19,21] Bryliakov and Talsi[22] showed that a simpler version of the Katsuki complexes is

[a] Centro Química Estrutural, Instituto Superior Técnico, TU Lisbon,
Av. Rovísco Pais, 1049-001 Lisboa, Portugal
[b] Departamento de Química Fundamental, Universidade da Coruña,
Campus de A Zapateira, 15071A Coruña, Spain
[c] TM-CNR sezione di Padova, Dipartimento di Scienze Chimiche, Università di Padova,
Via Marzolo 1, 35131 Padova, Italy
Supporting information for this article is available on the WWW under http://dx.doi.org/10.1002/ejic.201000792.

 WILEY ONLINE LIBRARY © 2010 Wiley-VCH Verlag GmbH & Co. KGaA, Weinheim

capable of catalyzing the asymmetric oxidation of sulfides to sulfoxides with H_2O_2 with simultaneous kinetic resolution of the sulfoxides. Optically active sulfoxides have been obtained with good-to-high enantioselectivities (up to 97% *ee*), but the overall yields and enantioselectivities are inferior to those obtained by the salen system of Katsuki and co-workers.[23]

In this paper we report the results of single-crystal X-ray diffraction analyses of a few salan ligands, the characterization of Ti–salan complexes, and their application as asymmetric catalysts in the sulfoxidation of sulfides in both organic solvents and in ionic liquids. Some of the ligands were also bound to cross-linked polystyrene to prepare the corresponding Ti^{IV} complexes and these heterogeneous complexes were also tested in sulfoxidation reactions.

Results and Discussion

Synthesis and Characterization of the Ligands and Complexes

Most of the ligands were prepared according to literature procedures in a two-step reaction: Condensation of the chiral diamine with 2 equiv. of aldehyde followed by reduction with $NaBH_4$. Their characterization has been presented in previous reports.[24,25] Ligand **5a** and complex **5** are new and their characterizations are reported below. For most of the ligands derived from cyclohexanediamine, crystals suitable for single-crystal X-ray diffraction studies were obtained and their structures are discussed below. The titanium(IV) complexes were prepared by the reaction of Ti^{IV}-(O*i*Pr)$_4$ with the ligands in methanol and their characterization by spectroscopic techniques is presented.

All of the Ti^{IV}–salan complexes **1**–**5** present ν(Ti–O) bands in the range 860–890 cm^{-1} (see Exp. Sect.). The ν(N–H) bands lie under broader bands centered at around 3400 cm^{-1} that arise from the presence of moisture in the solid samples. As expected for d^0 compounds, the electronic absorption spectra of the complexes show only bands in the UV region, which correspond to the π→π* transitions of the aromatic groups and are redshifted when compared with the spectra of the ligands.[24]

The electronic and circular dichroism spectra of complexes **1**–**3** are shown in Figure 1. Because Ti^{IV} has no d–d bands, there are no CD signals in the visible range. The Cotton effects observed are due to intraligand and CT bands and thus mostly show up in the UV range. The spectra of complexes **2** and **3** resemble mirror images of each other as they are complexes with ligands of opposite configurations of the stereogenic carbon atoms.

Most of the Ti–salan complexes characterized by X-ray diffraction studies are monomeric and show the ligand wrapped around the Ti in a *fac-fac* geometry. However, for the bulky complex derived from diphenyl diamine and 3,5-di-*tert*-butylsalicylaldehyde,[7] a dinuclear complex was obtained with a μ-oxo bridge between the titanium atoms, only one isopropoxo unit, and the ligand coordinated in a *fac-mer* fashion. Titanoxanes containing Ti_4O_4 units are

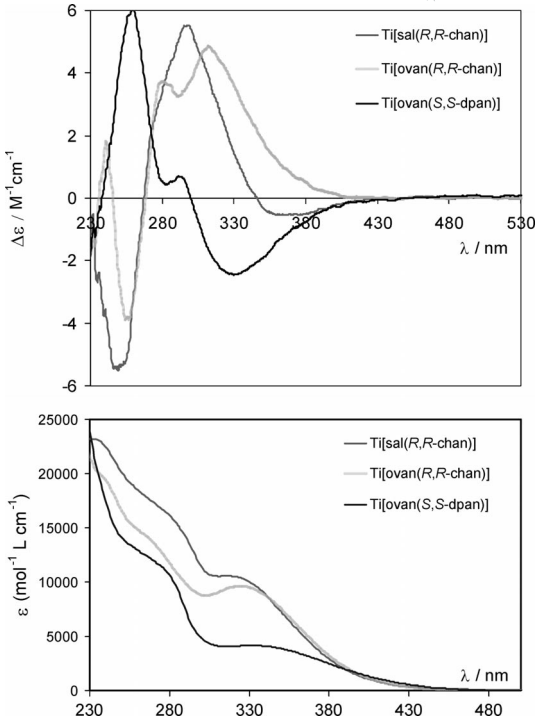

Figure 1. Circular dichroism and electronic spectra of complexes **1**–**3** in dichloromethane (DCM).

known and can be formed by controlled hydrolysis of the titanium species.[26–28] From solutions containing complex **1** we obtained an interesting tetranuclear structure bearing μ-oxo bridges between the titanium atoms and the ligand wrapped around the Ti also in a *fac-mer* geometry (see below). This resulted from the hydrolysis of the parent monomer.

Molecular Structures from Single-Crystal X-ray Diffraction Studies

The molecular structures of H_2sal(*R*,*R*-chan) (**1a**), H_2ovan(*S*,*S*-chan) (**2a**), and H_6pyr(*R*,*R*-chan)·4Cl^- (**4a**) were determined by single-crystal X-ray diffraction. ORTEP representations are presented in Figure 2 and selected bond lengths and angles are given in the Supporting Information. Ligands **1a** and **2a** show neutral structures and in **2a** one proton has migrated from one of the phenolate groups to one of the amine groups. Only half of the molecule of **4a** was found in the asymmetric unit, the inversion center being located at the midpoint of the cyclohexane ring. The molecule is tetracationic with all of the nitrogen atoms protonated and four chloride anions as counterions. In all of the structures the cyclohexane ring adopts the chair conformation and the NH–CH_2 (1.45–1.50 Å) and C–O distances (1.32–1.38 Å) are consistent with single-bond character. Overall, **1a**, **2a**, **4a**, and the previously reported salan ligands[24,25] are quite flexible molecules, which probably explains the rather moderate *ee* values obtained in the sulfoxidation reaction with Ti–salan complexes (see below). The molecular structures are discussed in the Supporting Information.

 © 2010 Wiley-VCH Verlag GmbH & Co. KGaA, Weinheim

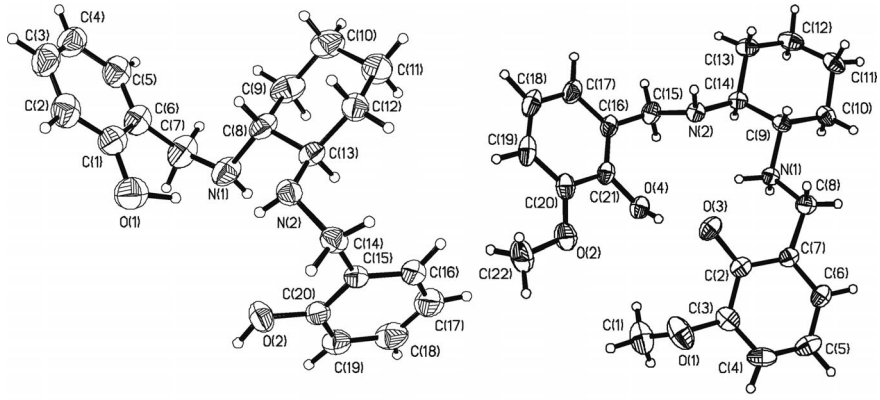

H_2sal(*R*,*R*-chan) **1a** H_2ovan(*S*,*S*-chan) **2a**

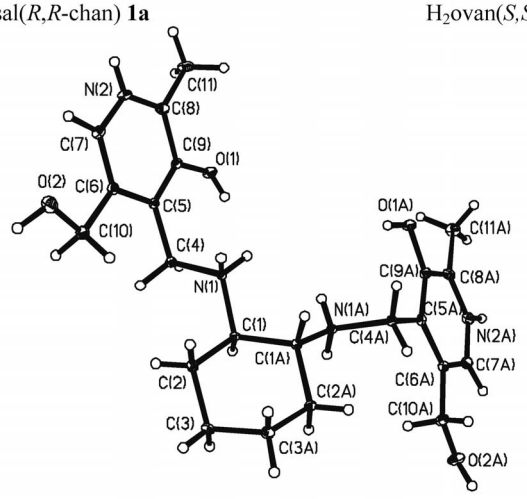

H_6pyr(R,R-chan)$^{4+}$ **4a**

Figure 2. ORTEP diagrams of H_2sal(*R*,*R*-chan) (**1a**), H_2ovan(*S*,*S*-chan) (**2a**), and H_6pyr(*R*,*R*-chan)$^{4+}$ (**4a**) with the thermal ellipsoids of the non-hydrogen atoms drawn at the 30% probability level. In the case of **4a** the solvent molecules and Cl^- anions have been omitted for clarity.

H_2sal(R,R-chan) (1a)

The asymmetric unit contains one neutral molecule. The structure is very distorted due to the large flexibility of the ligand, the torsion angles C(6)–C(7)–N(1)–C(8) and C(15)–C(14)–N(2)–C(13) being –68.91(32) and –54.94(21)°, respectively. The molecular structure of the same ligand but with two protons on each amine group and two Cl^- ions as counterions has been reported previously.[24]

H_2ovan(S,S-chan) (2a)

Figure 2 shows a representation of H_2ovan(*S*,*S*-chan). The asymmetric unit contains one neutral molecule of **2a** in which one proton has migrated from one of the phenolate oxygen groups to the closest amine atom. The molecule has a much more planar character than **1a**. The molecular structure of the compound is partly determined by intra- and intermolecular interactions involving hydrogen bonds (see Supporting Information), namely, strong intramolecular hydrogen bonds between the phenolate and amine groups.

H_6pyr(R,R-chan)$^{4+}$·4Cl$^-$·H_2O (4a)

The structure of **4a** is quite interesting because the molecule is tetraprotonated with the protons located on each of the nitrogen atoms. There are also four Cl^- ions and one water molecule. As a result of the protonation of the amine atoms there are no intramolecular hydrogen bonds between the phenolate oxygen (O_{phen}) and the amine nitrogen (N_{amine}) atoms, which in pyran [*N*,*N*′-ethylenebis(pyridoxylaminato)][10] conditioned the molecular structure. Overall, the geometrical parameters of pyr(*R*,*R*-chan) compare well with those obtained for pyran, although pyr(*R*,*R*-chan) shows a more distorted structure.

[Ti$_4${sal(R,R-chan)}$_4$(μ-O)$_4$] (1b)

The molecule is tetrameric with each monomer linked through a μ-oxo bridge and only half a molecule found in the asymmetric unit. An ORTEP diagram is depicted in Figure 3, and Table 1 includes selected bond lengths and angles. All monomers show *cis*-β geometry with the μ-oxo ligands occupying mutually *cis* coordination sites and the

 © 2010 Wiley-VCH Verlag GmbH & Co. KGaA, Weinheim

Table 1. Selected bond lengths [Å] and angles [°] for $[Ti_4\{sal(R,R\text{-chan})\}_4(\mu\text{-}O)_4]$ (**1b**).

Bond lengths [Å]				Bond angles [°]			
Ti(1)–O(6)	1.777(3)	O(2)–C(20)	1.320(4)	O(6)–Ti(1)–O(1)	102.52(13)	O(1)–Ti(1)–N(1)	85.64(13)
Ti(1)–O(1)	1.890(3)	N(2)–C(13)	1.480(5)	O(6)–Ti(1)–O(5)*	99.63(11)	C(20)–O(2)–Ti(1)	133.2(2)
Ti(1)–O(5)*	1.907(3)	N(2)–C(14)	1.488(5)	O(1)–Ti(1)–O(5)*	95.03(13)	C(13)–N(2)–Ti(1)	113.2(2)
Ti(1)–O(2)	1.962(3)	O(3)–C(21)	1.344(5)	O(6)–Ti(1)–O(2)	94.79(12)	C(14)–N(2)–Ti(1)	110.9(2)
Ti(1)–N(2)	2.204(4)	N(3)–C(27)	1.488(5)	O(1)–Ti(1)–O(2)	94.02(12)	Ti(2)–O(5)–Ti(1)*	147.27(18)
Ti(1)–N(1)	2.286(3)	N(3)–C(28)	1.500(5)	O(5)*–Ti(1)–O(2)	160.88(11)	Ti(1)–O(6)–Ti(2)	149.87(17)
O(1)–C(1)	1.327(5)	N(4)–C(34)	1.499(13)	O(6)–Ti(1)–N(2)	94.96(13)	O(5)*–Ti(1)–N(1)	81.54(12)
N(1)–C(7)	1.480(5)	N(4)–C(33)	1.500(5)	O(1)–Ti(1)–N(2)	162.22(13)	O(2)–Ti(1)–N(1)	82.239(11)
N(1)–C(8)	1.488(5)	O(4)–C(40)	1.027(14)	O(5)*–Ti(1)–N(2)	85.14(13)	N(2)–Ti(1)–N(1)	76.78(13)
				O(2)–Ti(1)–N(2)	81.14(11)	C(1)–O(1)–Ti(1)	137.9(3)
				O(6)–Ti(1)–N(1)	171.57(14)	C(8)–N(1)–Ti(1)	108.0(2)
				C(7)–N(1)–Ti(1)	112.7(2)		

* Symmetry transformations used to generate equivalent atoms in $[Ti_4\{sal(R,R\text{-chan})\}_4(\mu\text{-}O)_4]$ (**1b**): $-x + 0, -y + 1, z + 0$.

phenolate groups also mutually *cis*. Two monomers show Δ helicity and the other two Λ helicity. The titanium atoms adopt a very distorted octahedral geometry with each ligand acting as tetradentate through the two O_{phen} and the two N_{amine} atoms; The two bridging μ-oxo atoms complete the coordination sphere. The cyclohexane rings adopt a chair conformation with the asymmetric carbon atoms in *R* configuration. The Ti–μ–O(6)–Ti angle is 149.87(17)°. One of the Ti–μ-oxo bonds is stronger than the other: The one *trans* to the secondary amine groups shows π-bonding character with an average length of 1.777(3) Å, whereas the other is longer [1.884(3) Å]. The two Ti–O_{phen} bonds are also quite different with the bonds *trans* to the Ti–μ-oxo donors showing longer distances. The Ti(2)–O(4) bond length is abnormally long, 2.375(3) Å, possibly due to disorder in this phenolate ring that was not refined. In the Ti–N bonds this difference is not so noteworthy.

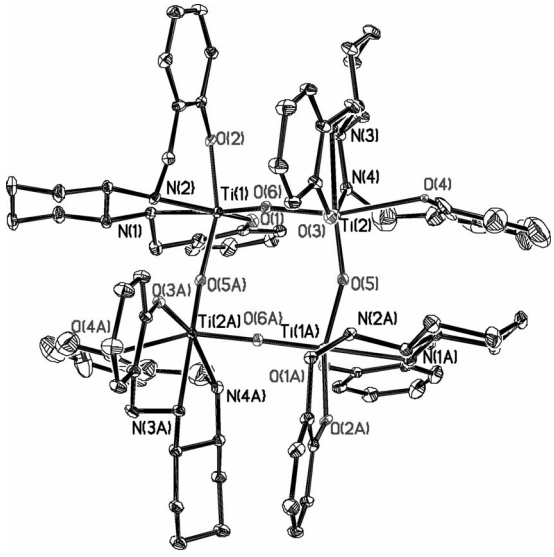

Figure 3. ORTEP diagram of $[Ti_4\{sal(R,R\text{-chan})\}_4(\mu\text{-}O)_4]$ (**1b**) with the atom-labeling scheme. The thermal ellipsoids of the non-hydrogen atoms are drawn at the 30% probability level. The hydrogen atoms and solvent molecules have been omitted for clarity.

The ligand molecules are quite distorted presenting two chelate rings (O_{phen}–N_{amine}–N_{amine}) in a plane [torsion angle C(6)–C(7)–N(1)–C(8) = –179.89(31)°] and the other chelate ring (amine, phenolate) roughly perpendicular to this [torsion angle C(15)–C(14)–N(2)–C(3) = 46.87(38)°]. Tetrameric structures have also been obtained with the maltolato and guaiacolato ligands $[Ti_4(maltolato)_8(\mu\text{-}O)_4]$[28] and $[Ti_4(guaiacolato)_8(\mu\text{-}O)_4]$.[26]

ESI-MS

ESI-MS experiments were conducted to investigate the nature of the titanium complexes in solution. The positive ion MS spectra collected for acidic samples (addition of 1% formic acid) of complexes **2** and **3** dissolved in CH_3CN/DCM (DCM = dichloromethane) show several intense peaks. Molecular ion peaks corresponding to the monomeric complexes were not observed in the MS spectra of either compound, all ion peaks corresponding to polymeric species and adducts with the formate anion (FA). For complex **2** the major peaks are assigned to $[Ti_2L_2O_2HK_2]^{3+}$ (*m*/*z* = 324.9), $[Ti_2L_2O_2H]^+$ (*m*/*z* = 897.4), and $[Ti_2L_2O(FA)]^+$ (*m*/*z* = 925.4). For complex **3** they are assigned to $[Ti_2L_2O_2HK_2]^{3+}$ (*m*/*z* = 324.9), $[Ti_2L_2O_2HNa_2(FA)]^{3+}$ (*m*/*z* = 495.4), and $[Ti_2L_2O_2K_3(2FA)]^+$ (*m*/*z* = 1013.5). These experiments indicate the aggregation of the complexes into structures containing at least two Ti–O units as a result of the hydrolysis of the parent isopropoxide complexes.

TGA Study

Thermogravimetric analysis under oxygen showed the high stability of [PS-PIP-Ti{5-MeO-sal(*R*,*R*-chan)}] (**6d**; see Scheme 4) up to around 230 °C. The first weight loss started above this temperature. Thereafter the complex decomposes in two steps but quantitative measurement of the weight loss in these steps was not possible due to their overlap. However, the stability of the final residue at a temperature greater than around 640 °C suggests the formation of TiO_2 and the metal loading was calculated from the mass of the final residue to be around 1.1 mmol Ti/g of resin.

Catalytic Studies: Asymmetric Sulfoxidation

The Ti complexes were screened for their potential as catalysts in the asymmetric sulfoxidation of thioanisole,

 © 2010 Wiley-VCH Verlag GmbH & Co. KGaA, Weinheim

used as a thioether model substrate (see Scheme 1). In all cases, the products were either (*R*)- or (*S*)-methyl phenyl sulfoxide and the sulfone resulting from the oxidation of the sulfoxides. In all the results presented, the percentage of sulfone is specified on a molar basis for these three products. A few control reactions were made to test the noncatalytic oxidation of thioanisole by H_2O_2 in the absence of a catalyst: The conversions were always very low after 24 h of reaction.

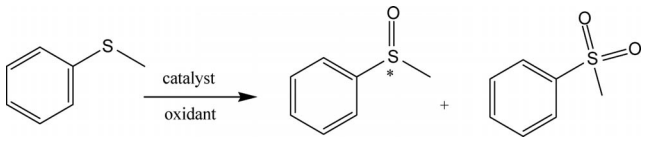

Scheme 1.

Several parameters were optimized, including catalyst concentration, temperature, and solvent. The results achieved after 24 h in 1,2-dichloroethane (DCE), acetone, and ethyl acetate are presented in Table 2. The best results were obtained with complex **1**, which bears no substituents on the aromatic rings. The use of complexes **2** and **3** led to lower sulfide conversion and enantioselectivity. With complex **1**, 0.25 mol-% catalyst loading was enough to obtain conversions higher than 94%, the enantioselectivity being 50% and with 13% of sulfone being formed (entry 2). The only effect observed upon decreasing the temperature to –10 °C (entry 5) was an increase in the formation of sulfone, but this has been ascribed to the higher concentration of oxidant used in this assay. This also suggests that the second oxidation step might affect the *ee* of the sulfoxide through kinetic resolution (see below).

Table 2. Sulfoxidation of thioanisole with titanium catalysts.[a]

Entry	Catalyst	n_{cat} [mmol]	Cat. [mol-%]	*T* [°C]	Conv. [%]	*ee* [%] (Config.)	Sulfone [%]
1	(*R*,*R*)-**1**	1.5×10^{-4}	0.015	0	16	8 (*R*)	0
2	(*R*,*R*)-**1**	2.4×10^{-3}	0.24	0	95	50 (*R*)	13
3	(*R*,*R*)-**1**	1.0×10^{-2}	1.0	0	94	51 (*R*)	16
4	(*R*,*R*)-**1**	5.0×10^{-2}	5.0	0	97	51 (*R*)	13
5[b]	(*S*,*S*)-**1**	1.0×10^{-2}	1.0	–10	94	51 (*S*)	23
6	(*R*,*R*)-**2**	1.0×10^{-2}	1.0	10	87	21 (*S*)	20
7	(*S*,*S*)-**3**	1.0×10^{-2}	1.0	10	86	8 (*S*)	20
8[c,d]	(*R*,*R*)-**1**	1.0×10^{-2}	1.0	0	84	38 (*R*)	14
9[d,e]	(*R*,*R*)-**1**	1.0×10^{-2}	1.0	0	88	46 (*R*)	27
10[d]	(*R*,*R*)-**5**	1.0×10^{-2}	1.0	0	87	41 (*R*)	14
11[c,d]	(*R*,*R*)-**5**	1.0×10^{-2}	1.0	0	37	16 (*R*)	1
12[c,d]	(*R*,*R*)-**5**	1.0×10^{-2}	1.0	25	63	38 (*R*)	7
13[d,e]	(*R*,*R*)-**5**	1.0×10^{-2}	1.0	0	88	47 (*R*)	23
14[c,d]	(*R*,*R*)-**6d**	6.6×10^{-2}	6.6	0	62	0	24
15[d,e]	(*R*,*R*)-**6d**	3.3×10^{-2}	3.3	0	60	0	23

[a] Unless otherwise stated: n_S = 1 mmol (S = substrate), $n_{H_2O_2}/n_S$ = 1.2, and reaction time = 24 h. [b] $n_{H_2O_2}/n_S$ = 1.5. [c] Solvent was acetone. [d] Slow addition of oxidant. [e] Solvent was ethyl acetate.

The kinetic profile was obtained in an experiment performed with 1 mol-% of (*R*,*R*)-**1**, 1 mmol of substrate, and 1.2 mmol of H_2O_2 (Figure 4). After around 2 h the reaction was almost complete and the enantioselectivity increased only slightly. Accumulation of the sulfone occurred at the expense of the *S*-sulfoxide. Thus, the kinetic resolution was confirmed by the direct oxidation of racemic methyl phenyl sulfoxide. The time evolution of the overall yields of sulfoxide and sulfone and the *ee* values of the sulfoxide are shown in Figure 5. After 1 h and with only 0.5 mmol of oxidant, the amount of sulfone was 47%. The *S* enantiomer of methyl phenyl sulfoxide is oxidized faster than the corresponding *R* enantiomer. These results are in agreement with those published by Bryliakov and Talsi,[22] who also observed a tandem process involving the oxidation of the sulfide and kinetic resolution of the sulfoxide mixtures. The same process has also been observed in the asymmetric sulfoxidation of thioanisole with V–salan complexes.[24]

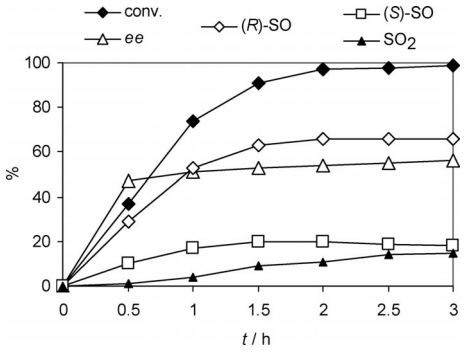

Figure 4. Profile of the sulfoxidation of thioanisole in DCE. Conditions: 1 mol-% of complex (*R*,*R*)-**1**, 1 mmol of substrate, 1.2 mmol of H_2O_2, and *t* = 0 °C; SO: sulfoxide; SO_2: sulfone.

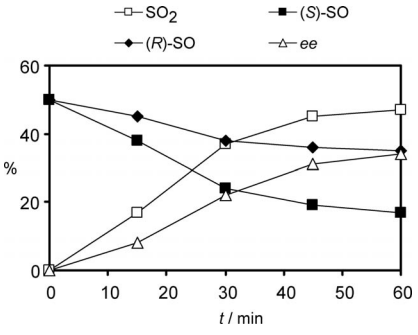

Figure 5. Kinetic resolution of racemic methyl phenyl sulfoxide in DCE. Conditions: 1 mol-% of complex (*R*,*R*)-**1**, 1 mmol of thioanisole, 0.5 mmol of H_2O_2, and *t* = 0 °C; SO: sulfoxide; SO_2: sulfone.

Because DCE is a volatile toxic solvent we decided to test the model catalytic reaction under other less hazardous conditions (see Table 2). However, the use of acetone (entry 8) led to a decrease in the conversion and enantioselectivity; the use of ethyl acetate (entry 9) had the same, but less pronounced effect, but the amount of sulfone formed was higher. The use of complex **5** in DCE (entry 10), acetone (entries 11 and 12), and ethyl acetate (entry 13) gave conversions and *ee* values lower than those found for complex **1** under similar conditions. Finally, the use of polystyrene-anchored complex **6d** either in acetone or in ethyl acetate gave moderate conversion, no enantioselectivity, and moderate amounts of sulfone (entries 14 and 15).

 © 2010 Wiley-VCH Verlag GmbH & Co. KGaA, Weinheim

We also tested the model reaction in environmentally benign solvents such as ionic liquids. Several ionic liquids (ILs) were prepared by standard procedures and used in the catalytic experiments. Although we tried to use a wide variety of ionic liquids some complexes were not soluble in some of the ionic liquids. Scheme 2 shows those in which the reactions were carried out and Table 3 reports the conditions and results obtained in each assay. Several control reactions were also carried out at room temperature, in the absence of catalyst, in different ILs, and under different conditions. All of the ILs tested in the absence of catalyst showed an ability to catalyze the oxidation of the sulfide to different extents, with $bmimNTf_2$ presenting a 45% yield in sulfoxide after around 24 h. Moreover, H_2O_2 seemed to be more active under the control reactions than *tert*-butyl hydroperoxide (TBHP). This result is very interesting and should be further explored as it shows that there may be potential in using neat chiral ionic liquids to carry out asymmetric catalysis.

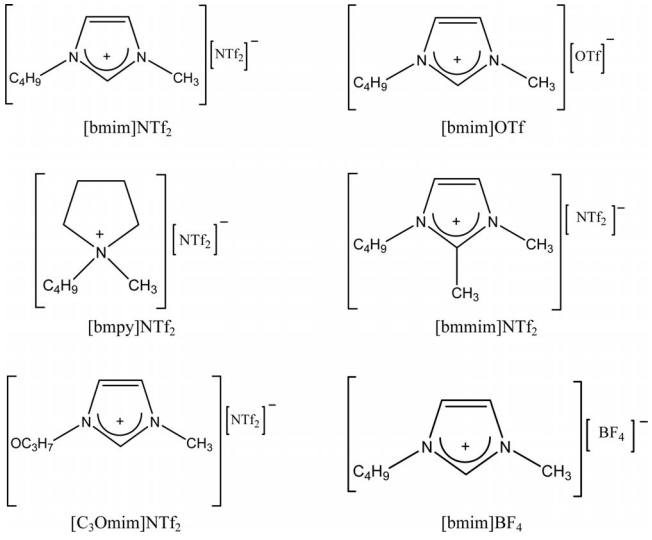

Scheme 2.

In a first screening we tested all of the complexes in ionic liquids containing the cation bmim at room temperature with 1 mol-% of catalyst and $n_{oxidant}/n_{substrate}$ (n_{Ox}/n_S) = 1.2. Because complex **4** is insoluble in all the ILs tested no other reactions were carried out with this complex. After 28 h, with $bmimBF_4$ the yields obtained were between 80–90% for the three complexes tested (see entries 5, 10, and 15). Unfortunately, in this IL no enantioselectivity was obtained.

Several oxidants were tested: Aqueous H_2O_2, TBHP and cumyl hydroperoxide (cumylHP). Their effect on the reaction outcome was tested with complexes **1**–**3** in $bmimNTf_2$ (entries 6–8 and 16–18) and TBHP was the one that showed the highest yields after 20 h at 0 °C and with complex **3** at room temperature. This may be due to the presence of water when using H_2O_2, which promotes the polymerization of the complexes with detrimental effects on the reaction rate and asymmetric induction. We can also observe that the catalyst with the best performance in terms of both activity

Table 3. Sulfoxidation of thioanisole using titanium–salan complexes as catalysts in ionic liquids.[a,b,c]

Entry	Complex	IL	Oxidant	n_{Ox}/n_S	T [°C]	t [h]	Conv. [%]	SO_2 [%]	*ee* [%]
1	–	$bmimNTf_2$	H_2O_2	1.2	25	22	45	2	nd
2	–	$bmpyNTf_2$	TBHP	1.2	25	20	12	0	nd
3	–	$bmpyNTf_2$	TBHP	0.5	25	22	8	0	nd
4	–	bmimOTf	H_2O_2	0.5	25	22	12	0	nd
5	**2**	$bmimBF_4$	H_2O_2	1.2	25	24	90	20	0
6	**2**	$bmimNTf_2$	H_2O_2	2	10	24	20	0	0
7	**2**	$bmimNTf_2$	cumylHP	2	10	24	35	1	6
8	**2**	$bmimNTf_2$	TBHP	2	10	24	50	1	4
10	**3**	$bmimBF_4$	H_2O_2	1.2	25	24	90	20	0
11	**3**	$bmimNTf_2$	H_2O_2	1.2	0	24	70	10	0
12	**3**	bmimOTf	H_2O_2	0.5	0	24	40	35	0
13	**3**	$bmimNTf_2$	cumylHP	1.2	25	18	5	0	0
14	**3**	$bmimNTf_2$	TBHP	1.2	25	18	30	16	0
15	**1**	$bmimBF_4$	H_2O_2	1.2	25	24	80	16	0
16	**1**	$bmimNTf_2$	H_2O_2	2	10	24	25	1	4
17	**1**	$bmimNTf_2$	cumylHP	2	10	24	45	10	19
18	**1**	$bmimNTf_2$	TBHP	2	10	24	100	10	19
19	**1**	$bbimNTf_2$	H_2O_2	0.5	25	24	80	2	12
20	**1**	$C_3OmimNTf_2$	H_2O_2	0.5	25	24	50	2	5
21	**1**	bm_2imNTf_2	H_2O_2	0.5	25	24	50	2	0
22	**1**	bmimOTf	H_2O_2	0.5	25	24	100	3	0
23	**1**	$bmpyNTf_2$	H_2O_2	0.5	25	24	80	1	10
24	**1**	$bmpyNTf_2$	TBHP	0.5	25	21	100	2	18
25	**1**	$bmpyNTf_2$	TBHP	0.5	0	20	14	0	7
26	**1**	$bmpyNTf_2$	TBHP	0.5	–10	23	6	0	nd

[a] Conditions: n_S = 1 mmol, catalyst = 1 mol-%. [b] The main product was the sulfoxide but in most cases some sulfone (SO_2) was obtained. [c] Two assays were performed with methyl *p*-tolyl sulfide as substrate in $bmimNTf_2$ (25 °C, n_{Ox}/n_S = 1.2, 22 h) and although high-to-moderate conversions of the sulfide was obtained (91% with TBHP and 54% with cumylHP), the *ee* values were low (18 and 3%, respectively) and high amounts of sulfone were also formed (7 and 18%, respectively).

 © 2010 Wiley-VCH Verlag GmbH & Co. KGaA, Weinheim

and asymmetric ability is complex (*R*,*R*)-**1** (see, e.g., entry 19). Therefore the catalytic parameters were optimized with this complex.

The solvent effect was tested by using complex **1** in different ILs with H_2O_2. In terms of activity bmimOTf was the best solvent (entry 22), but in terms of enantioselectivity (and high activity also) bbimNTf$_2$ showed the best performance although a moderate *ee* value was still obtained (entry 19).

In an attempt to increase the enantioselectivity we decreased the reaction temperature as often this improves the selectivity. However, as can be seen in Table 3, lowering the temperature led to a decrease in the *ee* values. A comparison of entries 23 and 24 once again confirms the better performance of TBHP in bmpyNTf$_2$ compared with H_2O_2. In two experiments performed with another substrate, methyl *p*-tolyl sulfide, a good yield and a moderate enantioselectivity were again obtained with TBHP, but this depends on a different stoichiometry.

Overall, from these preliminary catalytic experiments carried out with the ILs tested we can conclude that the best catalyst is complex **1**, without substituents on the aromatic rings, and the best conditions involve the use of NTf$_2$-based ionic liquids with TBHP as oxidant.

Another of our objectives was to study the effect of catalyst loading. However, owing to the low solubility of complex **1** in the IL, some experiments were carried out with 1:1 mixtures of bmpyNTf$_2$ and DCE. The kinetic profile is shown in Figure 6 and at 0 °C we can observe that the more catalyst, the slower the reaction, likely due to aggregation phenomena: DCE may not be enough to guarantee solubility.

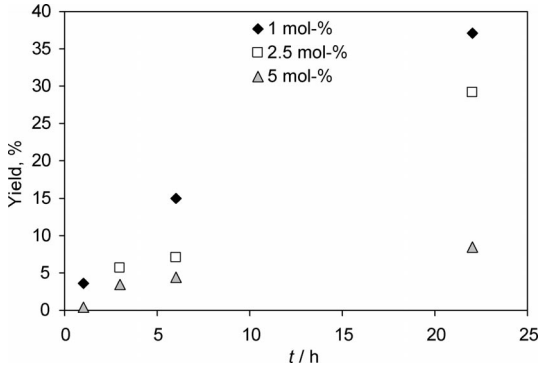

Figure 6. Time dependence of the yield of sulfoxide in the sulfoxidation of thioanisole in bmpyNTf$_2$/DCE (1:1) with complex (*R*,*R*)-**1**. Conditions: 1 mmol of thioanisole, 1 mmol of TBHP, and *t* = 0 °C.

By studying the reaction profile of the oxidation with TBHP in DCM and bmpyNTf$_2$ (Figure 7), it was found that the reaction is much faster in the IL than in the organic solvent. This is an interesting result because with H_2O_2 the reaction is faster in organic solvents. Indeed, the addition of water has been shown to reduce the catalytic oxidation in IL phases.[29]

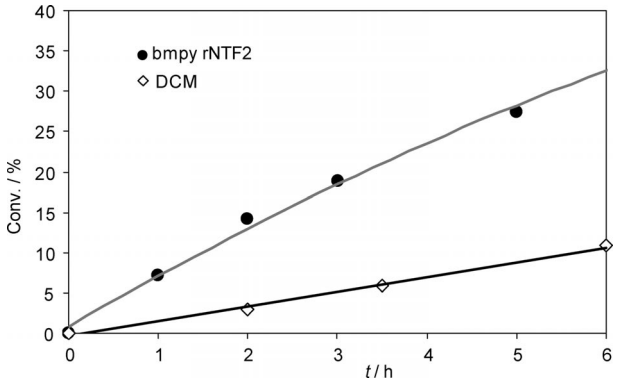

Figure 7. Time dependence of the conversion for the sulfoxidation of thioanisole in bmpyNTf$_2$ and DCM with complex (*R*,*R*)-**1**. Conditions: 1 mol-% of substrate, 0.5 mmol of TBHP, and *t* = 25 °C.

Conclusions

Several chiral salan compounds and the corresponding Ti–salan complexes have been synthesized and characterized. Namely, the crystal and molecular structures of H_2sal(*R*,*R*-chan) (**1a**), H_2ovan(*S*,*S*-chan) (**2a**), and H_6pyr(*R*,*R*-chan)$^{4+}$ (**4a**) were solved by X-ray diffraction methods, which showed the high flexibility of these ligands.

Upon dissolution in common organic solvents such as DCM, the Ti–salan compounds form polynuclear Ti(μ-O)-Ti species with binding modes involving the four donor atoms of the ligands and a μ-oxo bridge. The crystal and molecular structures of [Ti$_4${sal(*R*,*R*-chan)}$_4$(μ-O)$_4$] (**1b**) were also determined by single-crystal X-ray diffraction, which showed all Ti units with *cis*-β geometry and the μ-oxo ligands occupying mutually *cis* coordination sites.

The Ti–salan complexes were applied as catalysts in the sulfoxidation of thioanisole with H_2O_2 in DCE and showed high activities and moderate enantioselectivities for this process. Various parameters were tested such as different solvents, temperature, catalyst loading, catalyst concentration, rate of addition of oxidant, and phenol ring substituent effect on the overall conversion and enantioselectivity. The best catalyst is complex **1**, which bears no substituents on the aromatic groups of the ligand. The thioether conversion and selectivity of the formation of sulfoxide is good, but the enantioselectivity is rather low. Note that kinetic resolution occurs during the oxidation of the *R*- and *S*-sulfoxides formed. Namely, the methyl phenyl (*S*)-sulfoxide is oxidized faster to sulfone by catalyst **1** than the corresponding *R* enantiomer.

The polystyrene-anchored complex **6d**, with a [Ti{5-MeO-sal(*R*,*R*-chan)}] unit covalently bound to the polystyrene matrix through a piperazine matrix, showed good conversion, a moderate amount of sulfone formed, but no enantioselectivity. Further investigations will be aimed at exploring the use of the supported catalyst either in solids or in ILs in order to obtain an easily recyclable catalytic system.

The use of ionic liquids showed some limitations due to the rather low solubility of the catalysts. The conversions

 © 2010 Wiley-VCH Verlag GmbH & Co. KGaA, Weinheim

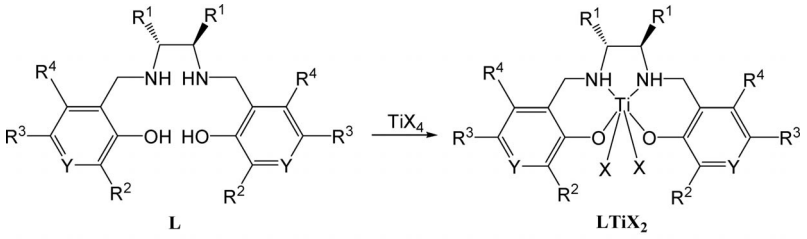

1: R^1 = -$(CH_2)_4$-, R^2 = H, R^3 = H, R^4 = H, X = *i*Pr-O , Y = C
2: R^1 = -$(CH_2)_4$-, R^2 = O-CH_3, R^3 = H, R^4 = H, X = *i*Pr-O, Y = C
3: R^1 = Ph, R^2 = O-CH_3, R^3 = H, R^4 = H, X = *i*Pr-O, Y = C
4: R^1 = -$(CH_2)_4$-, R^2 = CH_3, R^3 = H, R^4 = -CH_2OH, X = *i*Pr-O, Y = N
5: R^1 = -$(CH_2)_4$-, R^2 = H, R^3 = O-CH_3, R^4 = H, X = *i*Pr-O, Y = C

Scheme 3. Structural formulas of the chiral ligands and Ti complexes prepared.

were moderate and the enantioselectivities were rather low. Interesting results were found with mixtures of DCE and ILs and in the absence of catalyst that deserve further attention.

Experimental Section

Materials: Hydrogen peroxide, cumyl hydroperoxide, and *tert*-butyl hydroperoxide were obtained from Aldrich, thioanisole from Acros, and chloromethylated polystyrene (1.4–1.7 mmol Cl/g, cross linked with 1% divinylbenzene, 100–200 mesh) from Acros. All other chemicals were from Sigma–Aldrich.

Synthesis of Ligands: The ligands were synthesized following previously published procedures[24,25] (see Scheme 3). Single crystals suitable for X-ray diffraction studies were obtained for some of the ligands.

H_2sal(*R*,*R*-chan) (1a): Suitable crystals for X-ray diffraction studies were grown by slow evaporation of 2-propanol solutions: The ligand (ca. 0.1 g, free base or hydrochloride) was dissolved in 2-propanol (20 mL). This solution was left to evaporate in an open flask at room temperature for about four weeks. Colorless prisms were obtained.

H_2ovan(*S*,*S*-chan) (2a): The procedure was similar to the one used for the synthesis of **1a**. Colorless prisms were also obtained.

H_6pyr(*R*,*R*-chan)·4Cl^- (4a): Orange crystals were obtained from the slow evaporation (ca. 8 weeks) of an aqueous solution of the compound. Brown crystalline aggregates formed from the oily brown residue that remained.

$H_2$5-MeO-sal(*R*,*R*-chan) (5a): The procedure was similar to that used for the synthesis of **1a**. A pale-yellow solid was obtained; yield 89% (1.64 g). IR: $\tilde{\nu}$ = 3040 (C–H)$_{ar}$, 2947 and 2870 (C–H)$_{aliph}$, 1265 (C–O) cm^{-1}. ^{1}H NMR (400 MHz, [D$_4$]MeOH): δ = 1.45 (t, ^3J = 9.3 Hz, 2 H, CH_2), 1.74 (m, 2 H, CH_2), 1.87 (m, 2 H, CH_2), 2.44 (d, ^3J = 13 Hz, 2 H, CH_2), 3.63 (m, 2 H, CH_2CHNH), 3.75 (s, 6 H, $ArOCH_3$), 4.25 (s, 4 H, $ArCH_2NH$), 6.87 (s, 4 H, Ar), 7.13 (s, 2 H, Ar) ppm. $C_{22}H_{32}Cl_2N_2O_4$·MeOH (512.45): calcd. C 56.2, H 7.4, N 5.7; found C 56.1, H 7.5, N 5.3.

Synthesis of the Ti Complexes

[Ti{sal(*R*,*R*-chan)}] (1): $Ti^{IV}(OiPr)_4$ (1.1 g, 3.9 mmol) was added to a methanolic solution (25 mL) of sal(*R*,*R*-chan)·2HCl (1.7 g, 3.9 mmol) and the solution turned to orange. A 2 M aqueous solution of KOH was added dropwise until pH 7–8. A yellow solid precipitated after 15 min. Water (100 mL) was added and the solid was filtered and washed with water and *n*-hexane. The resulting yellow solid was then dissolved in CH_2Cl_2, filtered to remove any traces of TiO_2, and the solvent was evaporated. A yellow solid was obtained; yield 19%. IR: $\tilde{\nu}$ = 3246 (N–H), 3064 (C–H)$_{ar}$, 2931 and 2857 (C–H)$_{aliph}$, 1270 (C–O), 887 (Ti–O) cm^{-1}.$C_{20}H_{24}N_2O_3Ti$·CH_2Cl_2 (473.24; monomer): calcd. C 53.3, H 5.5, N 5.9; found C 53.7, H 5.9, N 6.0.

[Ti{ovan(*R*,*R*-chan)}] (2): The procedure was similar to the one used for the synthesis of **1**. A light-yellow solid was obtained; yield 21%. IR: $\tilde{\nu}$ = 3227 (N–H), 3058 (C–H)$_{ar}$, 2934 and 2859 (C–H)$_{aliph}$, 1278 and 1246 (C–O), 865 (Ti–O) cm^{-1}. $C_{22}H_{28}N_2O_5Ti$·1.5H_2O (475.38; monomer): calcd. C 55.6, H 6.6, N 5.9; found C 55.8, H 6.7, N 5.7.

[Ti{ovan(*S*,*S*-dpan)}] (3): The procedure was similar to the one used for the synthesis of **1**. The resulting orange-yellow oil obtained was "triturated" with THF, which was then removed and a yellow solid was obtained; yield 13%. IR: $\tilde{\nu}$ = 3227 (N–H), 3060, 3029, and 3004 (C–H)$_{ar}$, 2931 and 2836 (C–H)$_{aliph}$, 1248 (C–O), 866 (Ti–O) cm^{-1}. $C_{30}H_{30}N_2O_5Ti$·THF (618.57; monomer): calcd. C 66.0, H 6.2, N 4.5; found C 66.0, H 6.4, N 4.8.

[Ti{pyr(*R*,*R*-chan)}] (4): The procedure was similar to the one used for the synthesis of **1**, but performed with pyridoxal instead of salicylaldehyde. A light-yellow solid was obtained; yield 57%. IR: $\tilde{\nu}$ = 3216 (N–H), 2930 and 2860 (C–H)$_{aliph}$, 1248 (C–O), 887 (Ti–O) cm^{-1}. $C_{24}H_{36}N_4O_6Ti$·2H_2O (560.48; monomer): calcd. C 51.4, H 7.2, N 10.0; found C 51.6, H 7.2, N 9.6.

[Ti{5-MeO-sal(*R*,*R*-chan)}] (5): The procedure was similar to the one used for the synthesis of **1**. A bright-yellow solid was obtained; yield 68% (0.33 g). IR: $\tilde{\nu}$ = 3240 (N–H), 3028 (C–H)$_{ar}$, 2933 and 2857 (C–H)$_{aliph}$, 1263 and 1226 (C–O), 887 (Ti–O) cm^{-1}. $C_{44}H_{56}N_4O_{10}Ti_2$·3.5$H_2O$ (959.71; di-μ-oxo bridged dimer): calcd. C 55.1, H 6.6, N 5.8; found C 55.0, H 6.2, N 5.5.

Synthesis of Polystyrene-Anchored Compounds: Several polymer-anchored compounds were synthesized according to the procedure outlined in Scheme 4.

PS-Piperazine (PS-PIP) (6a): Chloromethylated polystyrene (3.2 g, 1.4 mmol Cl/g, 1% DVB, 100–200 mesh) was swollen in acetone for 30 min. Piperazine (0.6 g, 6.9 mmol) and K_2CO_3 (0.89 g, 6.4 mmol) were added to the polymer suspension. The mixture was stirred and heated at reflux for 3 d. The polymer beads were filtered and washed with water, acetone, and diethyl ether. The resin was dried under vacuum. Recovered mass: 3.35 g. Nitrogen anal. (for 100%

 © 2010 Wiley-VCH Verlag GmbH & Co. KGaA, Weinheim

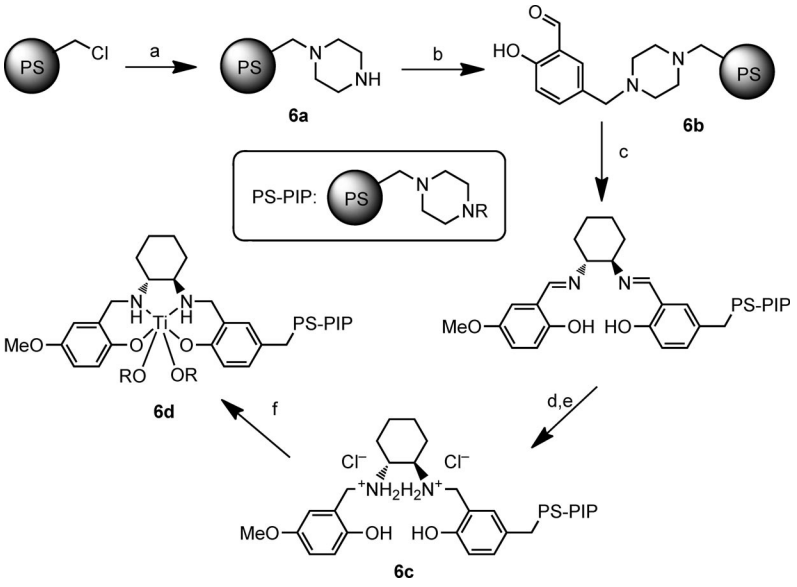

Scheme 4. Procedure for the synthesis of the polystyrene-anchored compounds. The process starts with the binding of a piperazine spacer and then the reaction with 5-(chloromethyl)salicylaldehyde. This was followed by the addition of the tartrate salt of (1*R*,2*R*)-cyclohexanediamine, reduction of the Schiff base compound obtained, and finally the binding of Ti to the anchored ligand. Reagents and conditions: a) piperazine, K_2CO_3, acetone, reflux, 72 h; b) 5-(chloromethyl)salicylaldehyde, K_2CO_3, THF, reflux, 72 h; c) (1*R*,2*R*)-cyclohexanediamine, 5-methoxysalicylaldehyde, THF/MeOH (1:1); d) $NaBH_4$, THF/MeOH/H_2O; e) HCl (pH ≈ 2); f) $Ti^{IV}(OiPr)_4$, H_2O.

substitution: 2.8 mmol N/g) N, 3.92%; found C 87.2, H 8.1, N 2.1 (ca. 1.5 mmol N/g, ca. 54% substitution of Cl).

PS-PIP-salicylaldehyde (6b): PS-Piperazine (PSPIP, **6a**; 2 g, 1.5 mmol N/g) was swollen in THF for 30 min. 5-(Chloromethyl) salicylaldehyde (0.7 g, 4.1 mmol) and K_2CO_3 (0.56 g, 4.1 mmol) were added to the polymer suspension. The mixture was stirred and heated at reflux for 3 d. The polymer beads were filtered, washed with water, acetone, and diethyl ether, and dried under vacuum. Recovered mass: 2.2 g. Elemental analysis: found C 88.4, H 8.1, N 1.9. IR: $\tilde{\nu}$ = 2845 $(C–H)_{aldehyde}$, 1653 (C=O), 1260 (C–O) cm^{-1}.

PS-PIP-5-MeO-sal(*R*,*R*-chan) (6c): PS-PIP-salicylaldehyde (**6b**; 1 g) was swollen in a mixture of THF/MeOH (1:1, 125 mL) for 30 min. The tartrate salt of (1*R*,2*R*)-1,2-cyclohexanediamine (0.37 g, 1.4 mmol) and K_2CO_3 (0.19 g, 1.4 mmol) in water (25 mL) were added to the polymer suspension. The mixture was stirred for around 24 h. Then 5-methoxysalicylaldehyde (0.21 g, 1.4 mmol, 0.17 mL) was added and the mixture was stirred for another 24 h. The bright-yellow polymer beads were filtered and washed with water, acetone, and diethyl ether. The resin was again suspended in THF/MeOH/H_2O (1:1:0.2) and $NaBH_4$ was added in excess. The mixture was stirred until the bright-yellow color had disappeared completely. The pH was adjusted with concd. aqueous HCl to around pH 2. The polymer beads were filtered and washed with water, THF, and diethyl ether. The resin was dried under vacuum. Recovered mass: 1.2 g. Elemental analysis: found C 82.2, H 7.9, N 2.0 (ca. 1.4 mmol N/g, ca. 54% substitution). IR: $\tilde{\nu}$ = 1267 (C–O) cm^{-1}.

[PS-PIP-Ti{5-MeO-sal(*R*,*R*-chan)}] (6d): PS-PIP-5-MeO-sal(*R*,*R*-chan) (**6c**; 0.62 g) was swollen in THF (100 mL) for 30 min. $Ti^{IV}(O-iPr)_4$ (0.35 g, 0.37 mL) was added to the polymer suspension. The mixture was stirred for 1 h. The polymer beads acquired a bright-orange color. Water was added and a suspension of TiO_2 formed readily. At this point the resin changed to a yellow color. The polymer beads were filtered through a coarse filter and washed with copious amounts of water. The resin was suspended in water and was subjected to an ultrasound bath for 15 min and then filtered again through a coarse filter until all TiO_2 (small particles) had been removed. The resin was washed with THF and diethyl ether and dried under vacuum. Recovered mass: 0.74 g. Elemental analysis: found C 82.2, H 7.9, N 2.0. IR: $\tilde{\nu}$ = 1265 (C–O) cm^{-1}. TGA indicates a titanium loading of 1 mmol Ti/g cm^{-1}.

Physical and Spectroscopic Studies: IR spectra were recorded with a BioRad FTS 3000 MX FTIR spectrometer. UV/Vis spectra were recorded with a Hitachi U-2000 spectrophotometer and the CD spectra with a Jasco J-715 spectropolarimeter. The ^1H NMR spectra were obtained with a Bruker Avance+ 400 Spectrometer. TGA was performed with a Perkin–Elmer STA 6000 thermal analyzer.

X-ray Crystal Structure Determinations: Three-dimensional X-ray data for compounds **1a** and **2a** were collected with a Bruker SMART 1000 CCD diffractometer, and for compounds **4a** and **1b** with a Bruker Kappa X8 Apex CCD diffractometer by using the θ–ω scan method. Data for **1a** and **2a** were collected at room temperature and for **4a** and **1b** at low temperature. Reflections were measured from a hemisphere of data collected of frames each covering 0.3° in ω. Of the 21185 reflections measured for **1a**, 24365 for **2a**, 6363 for **4a**, and 35147 for **1b**, all of which were corrected for Lorentzian and polarization effects and for absorption by semi-empirical methods based on symmetry-equivalent and repeated reflections, 2155, 3157, 2408, and 8408 independent reflections exceeded the significance level $|F|/\sigma(|F|) > 4.0$, respectively. Complex scattering factors were obtained by using the SHELXTL software package.[30] The structures were solved by direct methods and refined by full-matrix least-squares methods on F^2. Refinement converged with allowance for the thermal anisotropy of all the non-hydrogen atoms, except for O4 in **1b**. All the hydrogen atoms were left to refine freely in **1a**, **2a**, and **4a**, except for the hydrogen atoms of C21 and C22 in **2a** and of C11 in **4a**, which were included in calculated positions and refined by using a riding mode. For **1b**, all hydrogen atoms were included at calculated positions and refined

 © 2010 Wiley-VCH Verlag GmbH & Co. KGaA, Weinheim

Table 4. Crystal data, data collection and refinement data for compounds H_2sal(*R*,*R*-chan) (**1a**), H_2ovan(*S*,*S*-chan) (**2a**), H_6pyr(*R*,*R*-chan)$^{4+}$·4Cl$^-$·H_2O (**4a**), and [Ti_4{sal(*R*,*R*-chan)}$_4$(μ-O)$_4$] (**1b**).

	H_2sal(*R*,*R*-chan) (**1a**)	H_2ovan(*S*,*S*-chan) (**2a**)	H_6pyr(*R*,*R*-chan)·4Cl·H_2O (**4a**)	[Ti_4{sal(*R*,*R*-chan)}$_4$(μ-O)$_4$] (**1b**)
Formula	$C_{20}H_{26}N_2O_2$	$C_{22}H_{30}N_2O_4$	$C_{22}H_{38}Cl_4N_4O_5$	$C_{80}H_{96}N_8O_{12}Ti_4$
M_r	326.43	386.48	580.36	1553.25
Temperature [K]	293(2)	293(2)	100(2)	100(2)
Wavelength [Å]	0.71073	0.71073	0.71073	0.71073
Crystal system	orthorhombic	orthorhombic	monoclinic	tetragonal
Space group	*P*2(1)2(1)2(1)	*P*2(1)2(1)2(1)	*C*2	*I*4(1)
Unit cell dimensions				
a [Å]	10.046(4)	8.2903(4)	12.7428(5)	24.0490(4)
b [Å]	10.380(4)	11.2018(5)	9.7347(3)	24.0490(4)
c [Å]	17.683(6)	21.7422(11)	11.4164(4)	12.4115(5)
α [°]	90	90	90	90
β [°]	90	90	104	90
γ [°]	90	90	90	90
Volume [Å^3]	1844.0(11)	2019.12(17)	1374.18(8)	7178.2(3)
Z	4	4	2	4
Calcd. density [mg m^{-3}]	1.176	1.271	1.403	1.437
Absorption coefficient [mm^{-1}]	0.076	0.087	0.470	0.500
F(000)	704	832	612	3264
Crystal size [mm^3]	0.50 × 0.35 × 0.35	0.50 × 0.23 × 0.23	0.42 × 0.37 × 0.30	0.49 × 0.32 × 0.18
θ range for data collection [°]	2.33–28.33	1.87–28.31	1.84–28.29°	1.20–28.31
Index ranges	$-13 \le h \le 13$	$-10 \le h \le 11$	$-16 \le h \le 16$	$-32 \le h \le 26$
	$-13 \le k \le 13$	$-14 \le k \le 14$	$-6 \le k \le 12$	$-32 \le k \le 32$
	$-23 \le l \le 23$	$-28 \le l \le 28$	$-15 \le l \le 15$	$-16 \le l \le 16$
Reflections collected	21185	24365	6363	35129
Independent reflections	4451 [*R*(int) = 0.0589]	4932 [*R*(int) = 0.0473]	2437 [*R*(int) = 0.0145]	8897 [*R*(int) = 0.0292]
Completeness to θ = 28.33° [%]	97.70	99.30	99.10	99.7
Max. / min. transmission	0.9739 / 0.9630	0.9802 / 0.9576	0.8718 / 0.8270	0.9154 / 0.7911
Refinement method	full-matrix least squares on F^2	full-matrix least squares on F^2	full-matrix least squares on F^2	full-matrix least squares on F^2
Data/restraints/parameters	4451/0/321	4932/0/352	2437/1/224	8897/31/465
Goodness-of-fit on F^2	0.887	1.088	1.154	1.073
Final *R* indices [$I > 2\sigma(I)$]	R_1 = 0.0376	R_1 = 0.0443	R_1 = 0.0222	R_1 = 0.0571
	*wR*2 = 0.0791	*wR*2 = 0.0971	*wR*2 = 0.0614	*wR*2 = 0.1559
R indices (all data)	R_1 = 0.1147	R_1 = 0.0931	R_1 = 0.0229	R_1 = 0.0606
	*wR*2 = 0.0988	*wR*2 = 0.1207	*wR*2 = 0.0709	*wR*2 = 0.1592
Absolute structure parameter		0.4(13)	0.04(4)	0.05(3)
Extinction coefficient		0.0122(14)		
Largest diff. peak and hole [e Å^{-3}]	0.098 and –0.110	0.292 and –0.234	0.610 and –0.224	2.199 and –0.696

by using a riding mode. The absolute configurations of **2a**, **4a**, and **1b** were established by refinement of the enantiomorph polarity parameter [χ = 0.4(13) for **2a**, 0.04(4) for **4a**, and 0.06(3) for **1b**].[31,32] A final difference Fourier map showed no residual density outside 0.098 and –0.110 e Å^{-3} for **1a**, 0.292 and –0.234 e Å^{-3} for **2a**, 0.610 and –0.224 e Å^{-3} for **4a**, except for **1b**, 1.770 and –0.933 e Å^{-3}, which presents disorder in one phenolate ring that could not be refined. Crystal data and details on data collection and refinement are summarized in Table 4.

CCDC-783626 (for **1a**), -783627 (for **2a**), -783628 (for **1b**), and -783629 (for **4a**) contain the supplementary crystallographic data for this paper. These data can be obtained free of charge from the Cambridge Crystallographic Data Centre via www.ccdc.cam.ac.uk/data_request/cif.

Supporting Information (see also the footnote on the first page of this article): Crystal data, details of data collection and refinement, and discussion of the structures.

Acknowledgments

We wish to thank the Portuguese NMR Network (IST-UTL Center) for providing access to the NMR facilities and the Portuguese MS Network (IST Node) and Dr. Maria da Conceição Oliveira for the ESI measurements. We also thank the Programa Operacional Ciência e Inovação (POCI) 2010, Fundo Europeu de Desenvolvimento Regional (FEDER) and the Fundação para a Ciência e Tecnologia (FCT) (SFRH/BD/40279/2007, PTDC/QUI-QUI/112015/2009 and PTDC/QUI-QUI/098516/2008) for financial support as well as the Spanish-Portuguese Bilateral Programme (Acção Integrada E-56/05, Acción Integrada HP2004-00).

[1] P. Pitchen, H. B. Kagan, *Tetrahedron Lett.* **1984**, *25*,1049.
[2] S. H. Di Furia, G. Modena, G. Seraglia, *Synthesis* **1984**, *3*, 25.
[3] http://www.tytonis.com/esomeprazole.pdf.
[4] J. Balsells, P. J. Carroll, P. J. Walsh, *Inorg. Chem.* **2001**, *40*, 5568–5574.
[5] A. Cohen, A. Yeori, J. Kopilov, I. Goldberg, M. Kol, *Chem. Commun.* **2008**, 2149–2151.
[6] S. Gendler, A. L. Zelikoff, J. Kopilov, I. Goldberg, M. Kol, *J. Am. Chem. Soc.* **2008**, *130*, 2144.
[7] S. Groysman, E. Sergeeva, I. Goldberg, M. Kol, *Eur. J. Inorg. Chem.* **2005**, 2480–2485.
[8] A. Yeori, S. Groysman, I. Goldberg, M. Kol, *Inorg. Chem.* **2005**, *44*, 4466–4468.
[9] E. Y. Tshuva, N. Gendeziuk, M. Kol, *Tetrahedron Lett.* **2001**, *42*, 6405–6407.

 © 2010 Wiley-VCH Verlag GmbH & Co. KGaA, Weinheim

[10] I. Correia, J. Costa Pessoa, M. T. Duarte, R. T. Henriques, M. F. M. Piedade, L. F. Veiros, T. Jakusch, T. Kiss, I. Dornyei, M. C. M. A. Castro, C. F. G. C. Geraldes, F. Avecilla, *Chem. Eur. J.* **2004**, *10*, 2301–2317.
[11] I. Correia, J. Costa Pessoa, M. T. Duarte, M. F. M. Piedade, T. Jakusch, T. Kiss, M. C. M. A. Castro, C. F. G. C. Geraldes, F. Avecilla, *Eur. J. Inorg. Chem.* **2005**, 732–744.
[12] I. Correia, A. Dornyei, F. Avecilla, T. Kiss, J. Costa Pessoa, *Eur. J. Inorg. Chem.* **2006**, 656–662.
[13] I. Correia, A. Dornyei, T. Jakusch, F. Avecilla, T. Kiss, J. Costa Pessoa, *Eur. J. Inorg. Chem.* **2006**, 2819–2830.
[14] M. Shavit, D. Peri, C. M. Manna, J. S. Alexander, E. Y. Tshuva, *J. Am. Chem. Soc.* **2007**, *129*, 12098.
[15] A. J. Chmura, M. G. Davidson, M. D. Jones, M. D. Lunn, M. F. Mahon, A. F. Johnson, P. Khunkamchoo, S. L. Roberts, S. S. F. Wong, *Macromolecules* **2006**, *39*, 7250–7257.
[16] S. Gendler, S. Segal, I. Goldberg, Z. Goldschmidt, M. Kol, *Inorg. Chem.* **2006**, *45*, 4783–4790.
[17] Z. Y. Dai, C. J. Zhu, M. H. Yang, Y. F. Zheng, Y. Pan, *Tetrahedron: Asymmetry* **2005**, *16*, 605–608.
[18] Z. Y. Dai, M. R. Shao, X. S. Hou, C. J. Zhu, Y. H. Zhu, Y. Pan, *Appl. Organomet. Chem.* **2005**, *19*, 898–902.
[19] K. Matsumoto, Y. Sawada, T. Katsuki, *Pure Appl. Chem.* **2008**, *80*, 1071–1077.
[20] K. Matsumoto, Y. Sawada, T. Katsuki, *Synlett* **2006**, 3545–3547.
[21] Y. Shimada, S. Kondo, Y. Ohara, K. Matsumoto, T. Katsuki, *Synlett* **2007**, 2445–2447.
[22] K. P. Bryliakov, E. P. Talsi, *Eur. J. Org. Chem.* **2008**, 3369–3376.
[23] K. Matsumoto, B. Saito, T. Katsuki, *Chem. Commun.* **2007**, 3619–3627.
[24] I. Correia, P. Adão, M. R. Maurya, U. Kumar, F. Avecilla, R. T. Henriques, M. L. Kusnetzov, J. Costa Pessoa, *Pure Appl. Chem.* **2009**, *81*, 1279–1296.
[25] P. Adão, J. Costa Pessoa, R. T. Henriques, M. L. Kusnetzov, F. Avecilla, M. R. Maurya, U. Kumar, I. Correia, *Inorg. Chem.* **2009**, *48*, 3542–3561.
[26] P. Sobota, K. Przybylak, J. Utko, L. B. Jerzykiewicz, A. J. L. Pombeiro, M. F. C. G. da Silva, K. Szczegot, *Chem. Eur. J.* **2001**, *7*, 951–958.
[27] G. R. Willey, J. Palin, M. G. B. Drew, *J. Chem. Soc., Dalton Trans.* **1994**, 1799–1804.
[28] J. L. Lamboy, A. Pasquale, A. L. Rheingold, E. Melendez, *Inorg. Chim. Acta* **2007**, *360*, 2115–2120.
[29] S. Berardi, M. Bonchio, M. Carraro, V. Conte, A. Sartorel, G. Scorrano, *J. Org. Chem.* **2007**, *72*, 8954–8957.
[30] G. M. Sheldrick, *SHELXTL*, University of Göttingen, Göttingen, **1997**.
[31] H. D. Flack, G. Bernardinelli, *Acta Crystallogr., Sect. A* **1999**, *55*, 908–915.
[32] H. D. Flack, G. Bernardinelli, *Appl. Crystallogr.* **2000**, *33*, 1143–1148.

Received: July 21, 2010
Published Online: November 2, 2010

 © 2010 Wiley-VCH Verlag GmbH & Co. KGaA, Weinheim